PHYSICAL REVIEW B VOLUME 40, NUMBER 9 15 SEPTEMBER 1989-II

Photoemission and electronic structure of FeOOH: Distinguishing between oxide and oxyhydroxide

I. D. Welsh and P. M. A. Sherwood
Department of Chemistry, Willard Hall, Kansas State University, Manhattan, Kansas 66502

(Received 17 April 1989)

Valence-band and core x-ray-photoemission spectroscopy (XPS) has been used to examine the electronic structure of FeOOH and Fe_2O_3. The known small difference in the core-level Fe 2*p* spectra of the two compounds is discussed. $X\alpha$ calculations of an $FeO_6H_3{}^{3-}$ cluster are shown to give good agreement with the two-peak FeOOH valence-band XPS spectrum, and it is clear that FeOOH and Fe_2O_3 can be clearly distinguished in the valence-band region. $X\alpha$ calculations of an $FeO_6{}^{9-}$ cluster are found to predict the three-peak structure of the Fe_2O_3 valence band. The O 2*s* region of FeOOH is found to be more sensitive to chemical environment than the O 1*s* region, and the former region is well explained by the $X\alpha$ calculation. Little decomposition of FeOOH is found during data collection.

INTRODUCTION

The oxides and oxyhydroxides of iron have been the subject of many theoretical and experimental studies. These compounds are of wide importance and can occur in a variety of oxidation states and forms. In order to understand the corrosion of iron, and the action of corrosion inhibitors on an iron surface, the surface layer on iron needs to be examined and its chemistry understood. Photoemission has provided a powerful method for identification of the chemistry on iron surfaces, and a considerable amount of work has been reported on such surfaces. Wandelt[1] has reviewed the area, discussing the structure of the oxides and oxyhydroxides, their core and valence-band spectra, and the effectiveness of calculations in interpreting the results. A particular interest to us is the extent to which x-ray photoemission spectroscopy (XPS) can be used to distinguish between oxide and oxyhydroxide on an iron surface. This is because it is now widely recognized that oxyhydroxides play a very important role in the surface films on electrode and corrosion surfaces.[2]

In this paper we report the core and valence-band spectra of FeOOH and Fe_2O_3 and show that these compounds can be distinguished in the valence-band region. Such studies have already been reported by a number of workers (e.g., see the references in Refs. 1 and 3–24), but in this paper we report a study of the possible dehydration of FeOOH in the spectrometer, and the interpretation of the valence-band spectra of FeOOH and Fe_2O_3. We show that these compounds can be clearly distinguished in their valence-band region, and that this region can be effectively interpreted by $X\alpha$ cluster calculations.

EXPERIMENT

Our XPS measurements were made using a AEI ES200B spectrometer with a base pressure of better than 10^{-9} Torr using Mg $K\alpha$ X radiation. Spectra were recorded to achieve maximum instrument resolution (better than 0.8 eV) and data were usually collected with at least 17 points per eV in order to be sure to identify any subtle features that might be lost at lower resolution and a larger step size. Binding energies were calibrated using O 1*s* from oxide oxygen in the samples taken as 530.3 eV. Spectra were fitted using a nonlinear least-squares program with a 50% mixed Gaussian-Lorentzian product function.[25]

α-Fe_2O_3 and α-FeOOH samples were obtained from ALPHA as polycrystalline samples. Their purity was checked by powder x-ray diffraction using a Scintag instrument. No cleaning of the samples by Ar^+ etching was attempted in view of the decomposition that such a treatment is known to cause.[14,17–23] The O 1*s* spectrum of α-Fe_2O_3 showed a weak high-binding-energy shoulder at 531.5 eV in addition to the main peak at 530.3 eV. This feature was at comparable intensity to the feature assigned to nonstoichiometric surface oxygen atoms,[26] but it may also represent a trace of hydroxide.

RESULTS AND DISCUSSION

Figure 1 shows the Fe 2*p* core region of iron metal and α-Fe_3O_4, α-Fe_2O_3, and α-FeOOH. These spectra illustrate the main problem in using this spectral region for distinguishing between the oxides, namely the small differences between these compounds. Only slight improvement is obtained when monochromatized x rays are used to generate the spectra.[1,26,8] There is controversy in the literature as to the correct binding energies for these oxides, but it is generally agreed that the binding energies lie within 1 eV of each other. In the case of Fe_3O_4 separate components due to Fe(II) and Fe(III) have been identified.[1,26,8]

The distinction between an oxide and an oxyhydroxide is important in many situations. Clearly the O 1*s* region of the oxyhydroxide would be expected to show a doublet with one peak due to oxide and the other hydroxide. This is indeed found, but in general analytical situations

©1989 The American Physical Society

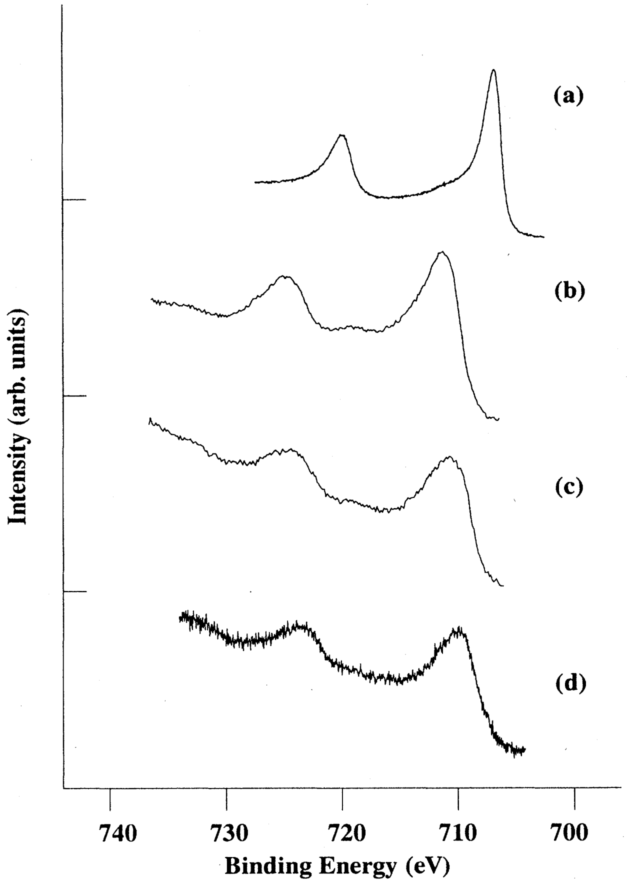

FIG. 1. Fe $2p$ core XPS spectra of iron compounds. (a) Iron metal (Fe $2p_{3/2}=706.8$ eV, FWHM$=1.1$ eV); (b) FeOOH (Fe $2p_{3/2}=711.4$ eV, FWHM$=4.7$ eV); (c) Fe_2O_3 (Fe $2p_{3/2}=710.7$ eV, FWHM$=4.7$ eV); (d) Fe_3O_4 (Fe $2p_{3/2}=710.1$ eV, FWHM$=4.8$ eV).

there are other compounds (such as water) that can give features in the O 1s hydroxide region. Another potential problem in this situation is the possible dehydration of the oxyhydroxide in the spectrometer. The potential for such decomposition, which will be partially instrument dependent (e.g., the heat from an x-ray gun can cause decomposition and the vacuum conditions will also be relevant) has to be considered in balancing the desire for ultra high-vacuum (UHV) conditions and long spectral collection times to achieve good statistics.

First we will discuss the information provided by the valence-band region, and then we will examine possible hydroxide dehydration during spectral collection, and finally we discuss the interpretation of the valence band region by $X\alpha$ calculations.

The valence-band region

The valence-band region of the iron oxides has received considerable attention, and in the case of the Fe(III) oxide and oxyhydroxide a clear difference is found.[1,26] We report the spectra of the oxide and oxyhydroxide in this region in order to compare our data with our calculations and to discuss the often-ignored O 2s spectral region.

An initial problem in examining this region in that the O 2s region is of comparable intensity to the rest of the valence band. This means that if nonmonochromatized x rays are used x-ray satellite radiation will give features in the normally discussed outer valence-band region. If uncorrected, these satellite features will be confused with genuine satellite features in the spectrum. Figures 2 and

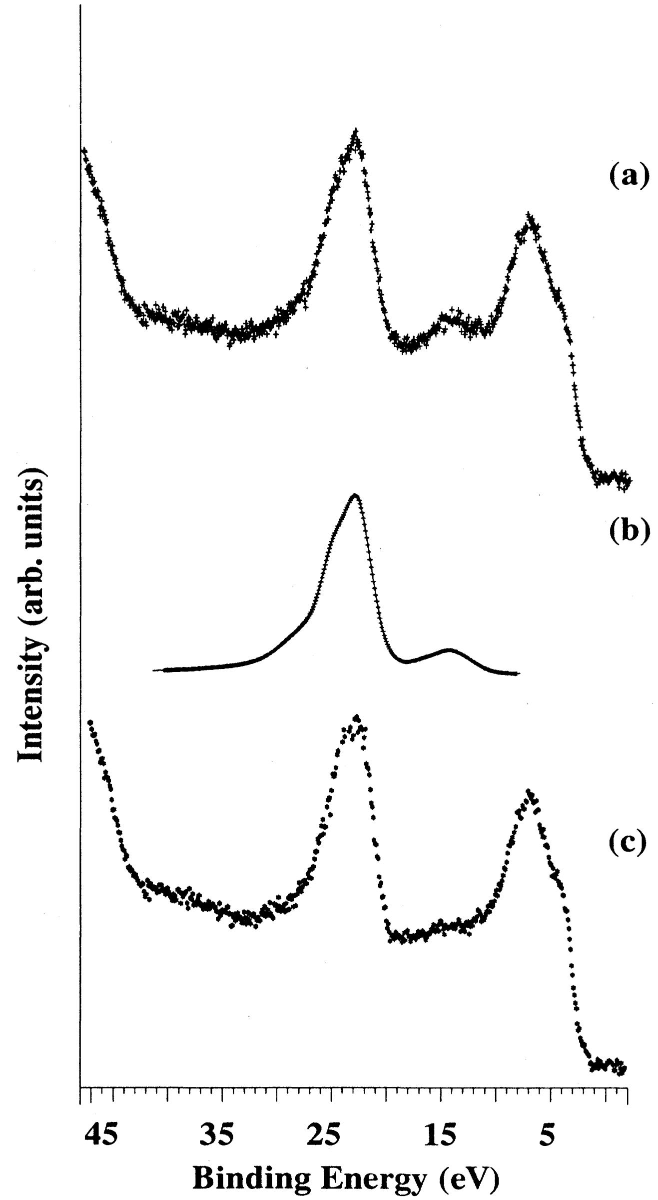

FIG. 2. Valence-band region of FeOOH. (a) Complete valence-band region; (b) spectrum synthesized to fit the O 2s region of the valence band, note the $\alpha_{3,4}$ x-ray satellite peak to higher binding energy; (c) the valence-band region of FeOOH after removal of the x-ray satellites from the O 2s region shown in (b).

3 show the importance of such x-ray-satellite–generated features for the Mg X radiation that we have used. The subtraction of such radiation-induced satellites shows that FeOOH has little satellite character and Fe_2O_3 a significant satellite feature. Other workers[7] have reported Fe_2O_3 valence-band data collected using unmonochromatized Mg X radiation, but have not discussed the role of overlapping radiation satellites. Clearly the neglect of the radiation-generated satellites would lead to substantial error in overestimating satellite intensity.

The subtraction process shown in Figs. 2 and 3 was carried out by fitting the O 2s region using Gaussian-Lorentzian peaks with each peak containing the Mg X radiation satellite features. The satellite features from the O 2s region so generated were then subtracted out from the valence-band spectrum.

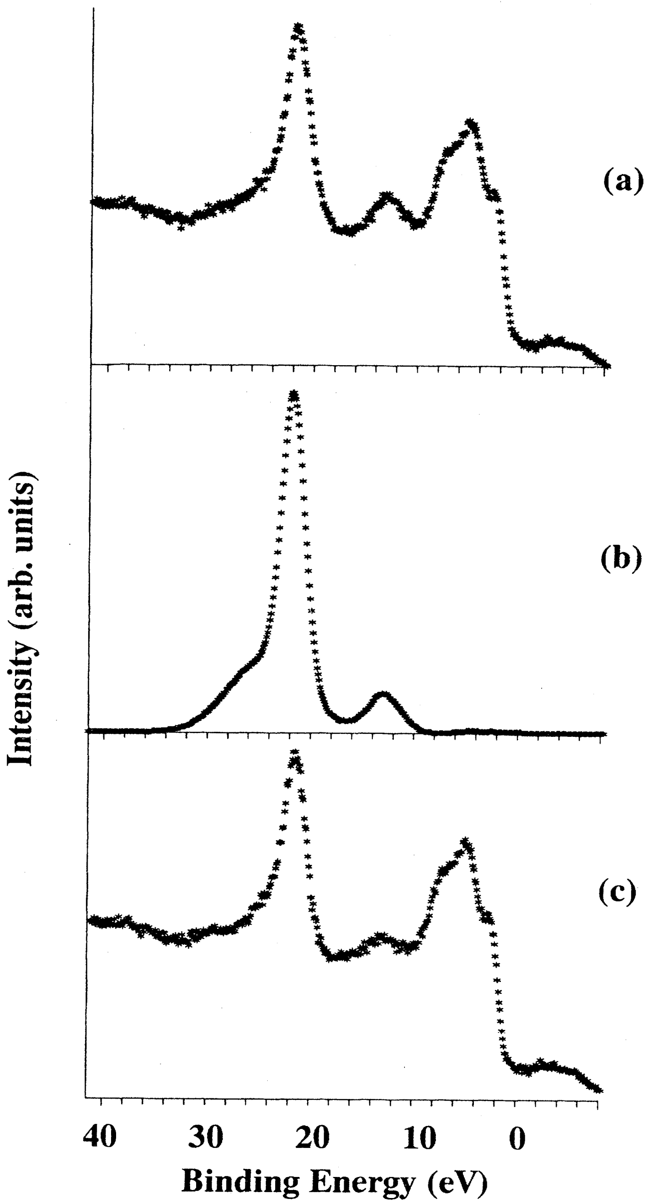

FIG. 3. Valence-band region of Fe_2O_3. (a) Complete valence-band region; (b) spectrum synthesized to fit the O 2s region of the valence band, note the $\alpha_{3,4}$ x-ray satellite peak to high binding energy; (c) the valence-band region of Fe_2O_3 after removal of the x-ray satellites from the O 2s region shown in (b).

The data in Figs. 2(c) and 3(c) will be used for comparison with the calculated spectra after removal of a nonlinear background.[27] The starting point of the nonlinear background at the high-binding side was adjusted to account for satellite intensity, especially for Fe_2O_3.

The O 2s region

The O 2s region is at a binding energy such that the molecular orbitals in compounds in this region contain a substantial amount of O 2s character. We have found this to be the case in a variety of rather different compounds.[28,29] The region is usually well separated from the rest of the valence-band region. This means that this region will show features more like a core region than a valence-band region, and in particular we might expect the O 2s region to show similarities with the O 1s region. However, we find[28,29] that this region shows a larger "chemical shift" than found in the O 1s region. Recently[30] the value of the O 2s region for giving corelike chemical-shift information from photoelectron spectra generated using synchrotron radiation has been discussed. We feel that the greater sensitivity of this region to chemical environment than the O 1s region makes this region valuable even when using conventional XPS.

Figure 4 shows the O 1s and O 2s regions of FeOOH.

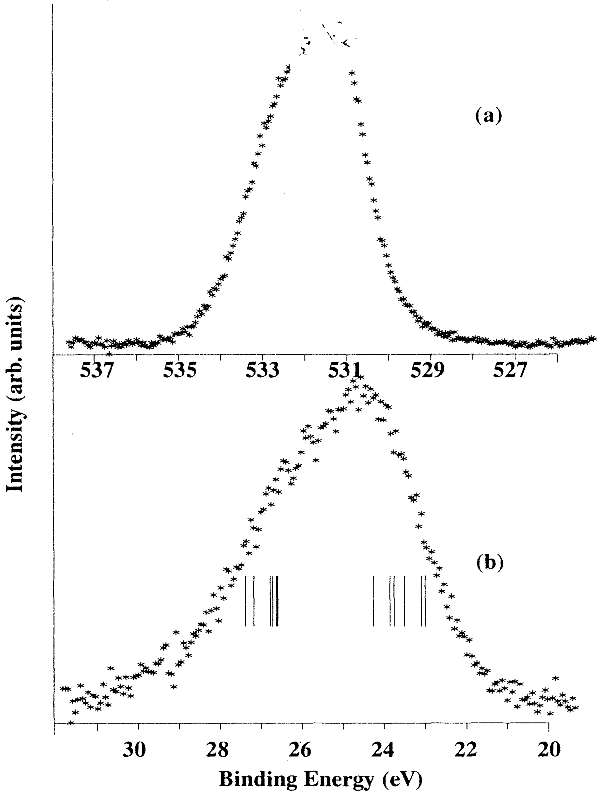

FIG. 4. Oxygen XPS regions of FeOOH. (a) O 1s region after about 15 h data collection; (b) O 2s region after about 15 h data collection with the positions of the O 2s levels from the $X\alpha$ calculation shown as a set of vertical lines.

It is clear that the separation of oxide and hydroxide features is greater in the O 2*s* than in the O 1*s* region. The O 2*s* region agrees well with the prediction of our $X\alpha$ calculation on a $FeO_6H_3^{3-}$ cluster, the energy-level positions for the OH^--type oxygen being shown as a cluster of lines at high-binding energy in Fig. 4(b) and those for O^{2-}-type oxygen being shown as a cluster of lines at lower binding energy.

Possible decomposition of FeOOH

Figures 5 and 6 show the O 1*s* and O 2*s* spectra of FeOOH after subjecting the sample to radiation for increasing longer periods of time. The higher kinetic energy of the O 2*s* electrons will mean that this region will be more bulk sensitive than the O 1*s* region. The simpler nature of the O 1*s* region means that it can be easily fitted to two overlapping peaks, one at 530.3 eV due to O^{2-} and another peak at 531.5 eV due to OH^-. It can be seen that there is some decomposition with time, but that this decomposition is not substantial. Quantification of this decomposition cannot easily be done exactly because one needs to make some assumptions as to the width of the O 1*s* component peaks. The fitted data illustrates the results when the widths are allowed to "float" (i.e., be evaluated by the curve-fitting process). Some change is also seen in the O 2*s* region, but likewise the change is not great with time. We thus conclude that the outer valence-band data for FeOOH can be collected for a substantial time (in order to obtain good statistics) without significant decomposition.

Interpretation of the outer valence-band region by $X\alpha$ calculations

We have used $X\alpha$ calculations to interpret the valence-band region of Fe_2O_3 and FeOOH. The parameters used and the features of the $X\alpha$ calculations are indicated in Table I. The geometry and bond lengths were taken from the well-known crystallographic information for these compounds.[31,32] Atomic spheres that overlapped by about 25% were used. There have been many previous $X\alpha$ calculations[33–36] for Fe_2O_3, and so the results of our calculation will not be discussed in detail. Most of the previous calculations[33–35] were ground-state calculations for touching spheres. We performed calculations on overlapping spheres and carried out a full set of transition-state calculations for each energy level in the outer valence-band region. We found little difference in the spectrum generated from the transition-state calculation (where half an electron is removed from each energy level to account for ionization) and the ground-state calculation. In the case of FeOOH only a ground-state calculation was performed, but we feel that the considerable extra computational time required for a full transition-state calculation for the large number of levels involved is not justified especially in light of the similarity of the transition-state calculation and ground-state results for Fe_2O_3. The low symmetry of the $FeO_6H_3^{6-}$ cluster required the calculation of all 88 energy levels (including 19 virtual levels).

Figure 7 shows the outer valence-band region for FeOOH after removal of the O 2*s* x-ray satellite features [i.e., Fig. 2(c) was used] compared with the result of the $X\alpha$ calculation. The calculated spectrum was obtained by fitting each energy level (or group of closely spaced energy levels) to a 50% Gaussian-Lorentzian product function,[25] with each peak having a full width at half max-

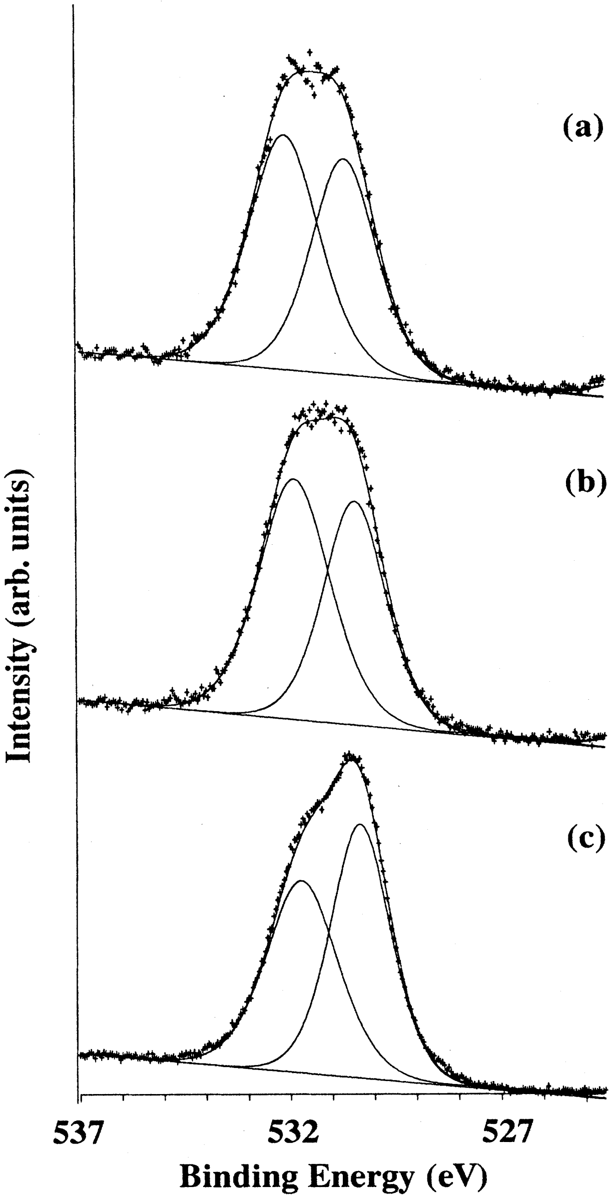

FIG. 5. O 1*s* region of FeOOH collected over increasing time periods to monitor dehydration. The high binding-energy peak is due to OH^- and the low-binding-energy (BE) peak is due to O^{2-} (set at 530.3 eV). The area ratio (hydroxide)/(oxide) is slowly reduced with time. (a) After 90 min data collection—area ratio 1.18 with peak widths: high BE $(OH^-)=1.98$ eV, low BE $(O^{2-})=1.81$ eV. (b) After 260 min data collection—area ratio 1.23 with peak widths: high BE $(OH^{2-})=2.01$ eV, low BE $(O^{2-})=1.75$ eV. (c) After 1095 min data collection—area ratio 0.90 with peak widths: high BE $(OH^-)=2.02$ eV, low BE $(O^-)=1.69$ eV.

imum (FWHM) of 2 eV and an area given by the sum of each level's atomic population multiplied by its atomic photoelectron cross section.[37] The atomic populations used for the component peak areas were adjusted for the stoichiometry FeOOH (rather than the cluster stoichiometry $FeO_6H_3^{3-}$). Excellent agreement is obtained between theory and experiment, and the two-peak characteristics of the FeOOH outer valence-band region are accurately explained. We were interested to find out whether it was the presence of the hydrogen atoms or just the lowering of symmetry from an idealized octahedral FeO_6^{9-} cluster used for Fe_2O_3 that caused the change in the two-peak outer valence-band region of FeOOH from the three-peak outer valence-band region of Fe_2O_3. We thus performed a calculation for an FeO_6^{9-} cluster with the C_{2v} symmetry of FeOOH. Oxygen sphere radii of 1.06 Å (OH−1), 1.22 Å (OH−2), 1.26 Å (O−3), and 1.35 Å (O−4) were used with all other parameters (except for the absence of hydrogen) the same as the $FeO_6H_3^{3-}$ cluster (Table I). This cluster gave a predicted spectrum very similar to that for Fe_2O_3 shown in Fig. 8. Further the O 2*s* region showed the most widely separated levels to be separated by 2.05 eV in contrast to the $Fe_2O_6H_3^{6-}$ cluster where these levels were separated by 4.52 eV. We can thus conclude that the hydrogen atoms sufficiently perturb the electron density around the oxygen that a significant valence-band spectral difference occurs. This suggests that the valence-band region promises to be a fruitful method for distinguishing between oxide and hydroxide.

Figure 8 shows the outer valence-band region for Fe_2O_3 after removal of the O 2*s* x-ray satellite features [i.e., Fig. 3(c) was used] compared with the result of our

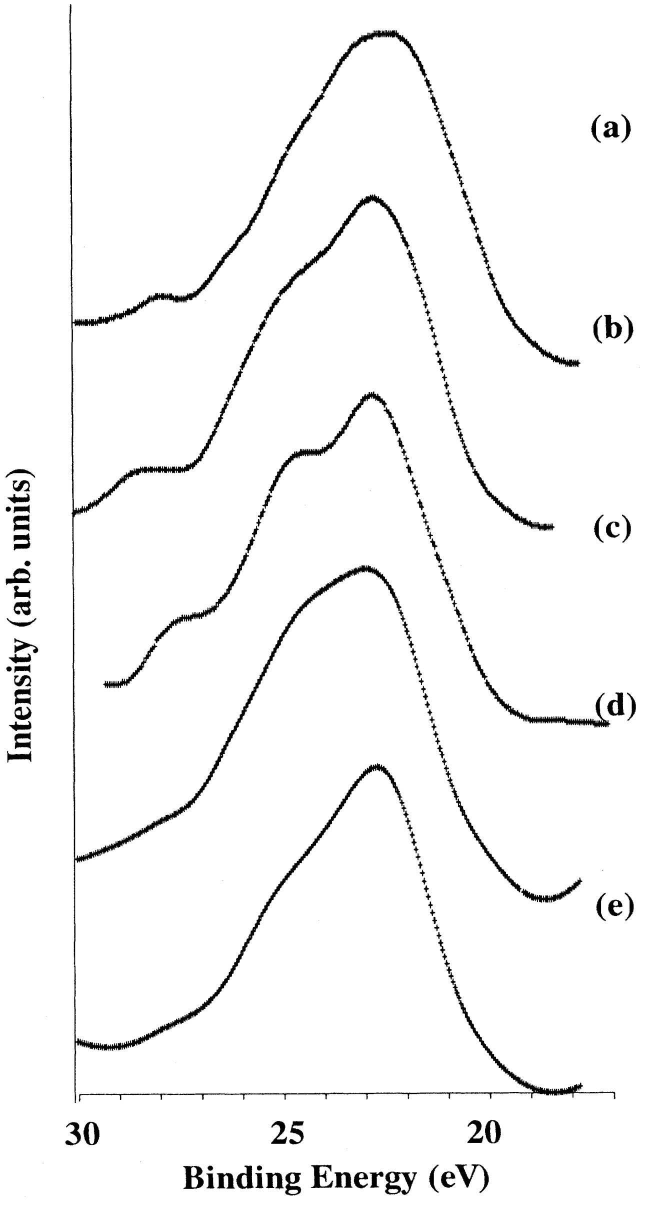

FIG. 6. O 2*s* region of FeOOH collected over increasing time periods to monitor dehydration. Spectra were smoothed with a quartic-quintic smooth repeated 80 times, the smoothing interval was 0.7×FWHM. (a) After 50 min data collection, (b) after 80 min data collection, (c) after 120 min data collection, (d) after 240 min data collection, and (e) after 990 min data collection.

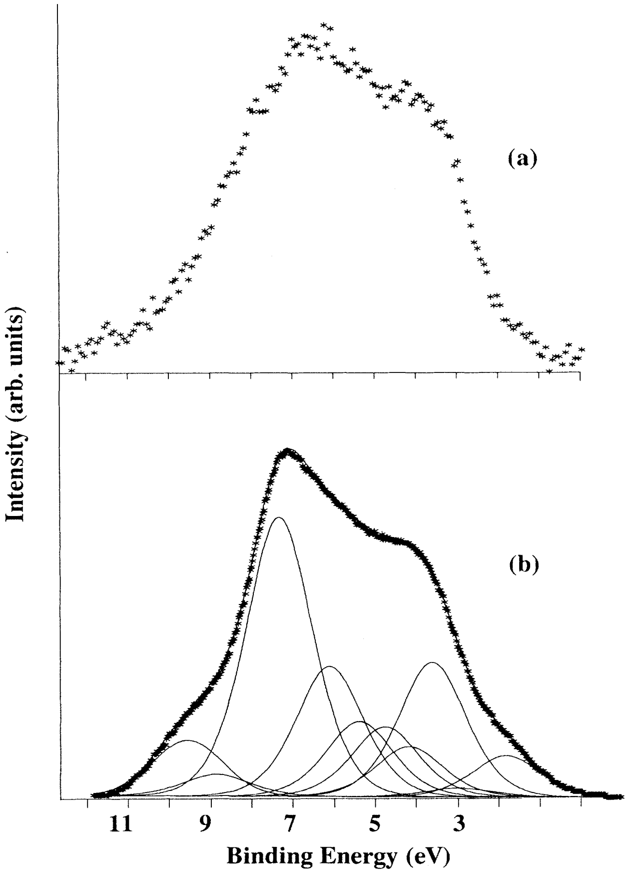

FIG. 7. Outer valence-band spectrum of FeOOH. (a) Experimental spectrum after removal of O 2*s* region as in Fig. 2(c), together with a nonlinear background removal. (b) Spectrum calculated from the ground-state *Xα* calculation.

TABLE I. Parameters used and features of the $X\alpha$ calculations.

α values: iron 0.7115, oxygen 0.7445, outer 0.7380,
hydrogen 0.7765, intersphere 0.7370
Maximum l value: iron 2, oxygen 1, hydrogen 0

Cluster:	FeO_6^{9-}	$FeO_6H_3^{3}$
Symmetry	O_h	C_{2v}
Fe—O bond lengths:	2.03 Å	1.89 Å (OH−1), 2.02 Å (OH−2) 2.05 Å (O−3), 2.12 Å (O−4)
O—H bond lengths:		1.00 Å
Iron sphere radius:	1.30 Å	1.31 Å
Oxygen sphere radius:	1.24 Å	0.74 Å (OH−1), 0.88 Å (OH−2) 0.85 Å (O−3), 0.98 Å (O−4)
Hydrogen sphere radius:		0.37 Å
Watson sphere radius:	2.03 Å	2.04 Å
Outer sphere radius	3.27 Å	3.49 Å
Virial ratio $(-2T/V)$:	1.002 11	1.002 62
Convergence:	When the difference in potentials at the beginning and end of the iteration were less than 10^{-5} of the potential at the start of the iterations. This gives energy levels that differed by less than 10^{-6} Ry between the last two iterations	
Core electrons:	"Thawed" so that they retained atomic character while being fully included in the iterative process. Fe 1s, 2s, and 2p electrons and O 1s electrons were treated as core electrons	

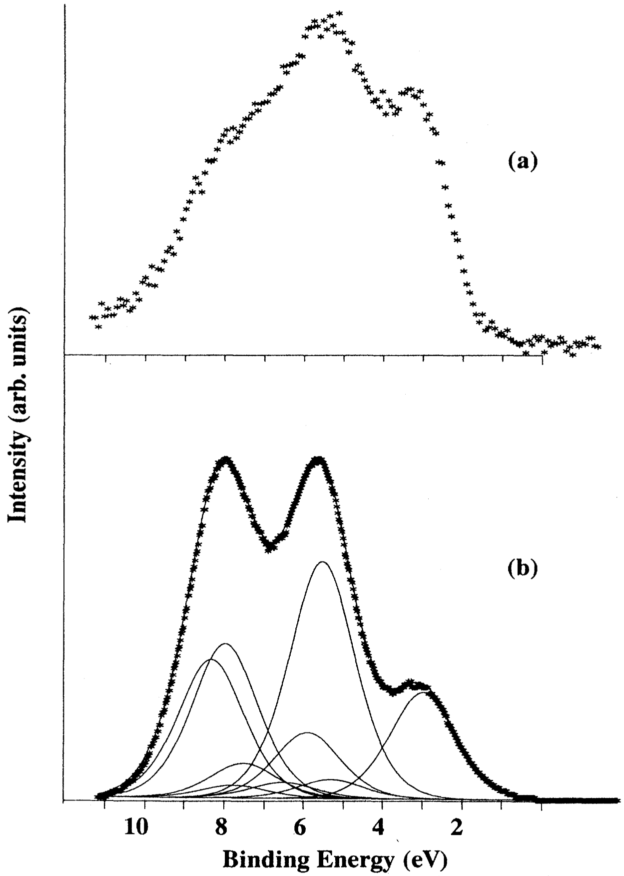

FIG. 8. Outer valence-band spectrum of Fe_2O_3. (a) Experimental spectrum after removal of O 2s region as in Fig. 3(c), together with a nonlinear background removal. (b) Spectrum calculated from the ground-state $X\alpha$ calculation.

ground-state $X\alpha$ calculation. The calculated spectrum was obtained using the same method described for FeOOH above. In this case the three-peak structure of the Fe_2O_3 spectrum is accurately predicted, with peak positions close to experimental values. The relative peak intensities are such that the highest binding-energy peak is too intense and the lowest binding-energy peak is not intense enough when compared with the experimental spectrum. The experimental spectrum has had a nonlinear background removed using the previously described method.[27] Any background removal method has some error associated with it, so there is some uncertainty regarding relative intensities. Another possible source of error is that we have modeled Fe_2O_3 to an octahedral FeO_6^{9-} cluster whereas the actual crystal structure of Fe_2O_3 consists of two trigonally distorted FeO_6 octahedra sharing a three-oxygen face. Nagel[36] has reported an $X\alpha$ calculation for a $Fe_2O_9^{12-}$ cluster consisting of these two FeO_6 octahedra. We have examined Nagel's data and find that this gives a better fit to the experimental intensity ratios for the three peaks. Previous[33–36] $X\alpha$ calculations for FeO_6^{9-} give similar energies to our calculation, though the atomic populations were not published and so could not be compared with our data. Atomic populations are important in predicting XPS data due to the substantial differences in photoelectric cross section between oxygen and iron orbitals.

CONCLUSIONS

We report the first calculation of the FeOOH valence-band spectrum. We find that this $X\alpha$ calculation gives excellent agreement with the experimental valence-band spectrum (including the O 2s region). For comparison we find that $X\alpha$ calculations (both ours and previously published calculations) predict the three-peak outer valence-band region of Fe_2O_3. It should be pointed out that these calculations (in contrast to other types of calculation that have been used to predict iron oxide valence bands) do not contain any parametrization to the experimental data. The agreement between the $X\alpha$ calculations and experiment, especially for FeOOH, shows that they form a reasonable basis for predicting the spectral features. In particular the results suggest that oxides and oxyhydroxides may in general be distinguished in the valence-band region.

This system also shows, as we have found in other compounds, that the O 2*s* region, while being rather core-like, is more sensitive to changes in chemical bonding than the O 1*s* region. It is also more bulk sensitive, which can be useful in cases where potential compound decomposition is a problem.

ACKNOWLEDGMENTS

We are grateful to International Paint plc for financial support, and to the U.S. Department of Defense for funding the x-ray diffraction equipment.

---

[1] K. Wandelt, Surf. Sci. Rep. **2**, 1 (1982).
[2] P. M. A. Sherwood, Chem. Soc. Rev. **14**, 1 (1985).
[3] N. S. McIntyre and D. G. Zetaruk, Anal. Chem. **49**, 1521 (1977).
[4] D. T. Harvey and R. W. Linton, Anal. Chem. **53**, 1684 (1981).
[5] G. Grenet, Y. Jugnet, Tran Minh Duc, and M. K. Kibler, J. Chem. Phys. **72**, 218 (1980).
[6] A. Fujimori, N. Kimizuka, M. Taniguchi, and S. Suga, Phys. Rev. B **36**, 6691 (1987).
[7] A. Fujimori, M. Saeki, M. Taniguchi, and S. Suga, Phys. Rev. B **34**, 7318 (1986).
[8] G. C. Allen, P. M. Tucker, and R. K. Wild, Philos. Mag. **46**, 411 (1982).
[9] N. Beathan, A. F. Orchard, and G. Thornton, J. Phys. Chem. Solids **42**, 1051 (1981).
[10] G. Grenet, Y. Jugnet, Tran Minh Duc, and M. Kibler, J. Chem. Phys. **74**, 2163 (1981).
[11] D. D. Dawn and B. M. DeKoven, Surf. Interface Anal. **10**, 63 (1987).
[12] H. Kato, T. Ishii, S. Masuda, Y. Harada, T. Miyano, T. Komenda, M. Onchi, and Y. Sakisaka, Phys. Rev. B **32**, 1992 (1985).
[13] S. Masuda, Y. Harada, H. Kato, K. Yagi, T. Komeda, T. Miyano, M. Onchi, and Y. Sakisaka, Phys. Rev. B **37**, 8088 (1988).
[14] J. F. van Acker, Z. M. Stadnik, J. C. Fuggle, H. J. W. M. Hoekstra, K. H. J. Buschow, and G. Stroink, Phys. Rev. B **37**, 6827 (1988).
[15] R. L. Kurtz and V. E. Henrich, Phys. Rev. B **36**, 3413 (1987).
[16] K. Hirokawa and Y. Danzaki, Surf. Interface Anal. **4**, 63 (1982).
[17] M. Hendewerk, M. Salmeron, and G. A. Somorjai, Surf. Sci. **172**, 544 (1986).
[18] D. R. Baer and M. T. Thomas, Appl. Surf. Sci. **26**, 150 (1986).
[19] P. Mills and J. L. Sullivan, J. Phys. D **16**, 723 (1983).
[20] R. J. Lad and V. E. Henrich, Surf. Sci. **193**, 81 (1988).
[21] E. Paparazzo, Surf. Sci. **200**, L470 (1988).
[22] R. J. Lad and V. E. Henrich, Surf. Sci. **200**, L473 (1988).
[23] E. Paparazzo, Appl. Surf. Sci. **25**, 1 (1986).
[24] M. Aeschlimann, G. L. Bona, F. Meier, M. Stampanoni, and G. Zampieri, Helv. Phys. Acta **60**, 794 (1987).
[25] P. M. A. Sherwood, in *Practical Surface Analysis by Auger and X-ray Photoelectron Spectroscopy,* edited by D. Briggs and M. P. Seah (Wiley, New York, 1983), Appendix 3.
[26] C. R. Brundle, T. J. Chang, and K. Wandelt, Surf. Sci. **68**, 459 (1977).
[27] A. Proctor and P. M. A. Sherwood, Anal. Chem. **54**, 13 (1982).
[28] Y. Xie and P. M. A. Sherwood, Chem. Mater. **1**, 427 (1989).
[29] P. M. A. Sherwood (unpublished).
[30] W. Ranke and H. J. Kuhr, Phys. Rev. B **39**, 1595 (1989).
[31] R. L. Blake, T. Zoltai, R. E. Hessevick, and L. W. Finger, U. S. Bur. Mines Rep. Invest. No. 7384, 1970 (unpublished).
[32] R. W. G. Wyckoff, *Crystal Structure,* 2nd ed. (Interscience, New York, 1963), Vol. 1.
[33] J. A. Tossell, D. J. Vaughan, and K. H. Johnson, Nature Phys. Sci. **244**, 42 (1973).
[34] J. A. Tossell, D. J. Vaughan, and K. H. Johnson, Am. Mineral. J. **59**, 319 (1974).
[35] J. A. Tossell, Am. Mineral. J. **61**, 130 (1976).
[36] S. Nagel, J. Phys. Chem. Solids **46**, 905 (1985).
[37] J. H. Scofield, J. Electron Spectrosc. **8**, 129 (1976).